HIGHLY FOLDABLE THIN-PLY STRUCTURES LEVERAGING GLASS FIBER ELASTICITY

M. J. Chen[1*], G. A. Pappas[1], N. Cesarovic[2,3], V. Falk[2,3,4] and P. Ermanni[1]
[1] Laboratory of Composite Materials and Adaptive Structures, Department of Mechanical and Process Engineering, ETH Zurich, Switzerland
[2]Translational Cardiovascular Technologies, ETH Zürich, Switzerland
[3]Klinik für Herz-, Thorax- und Gefäßchirurgie, Deutsches Herzzentrum Berlin, Germany
[4]Klinik für Kardiovaskuläre Chirurgie, Charité Universitätsmedizin Berlin, Germany
* Corresponding author (jichen@ethz.ch)

Keywords: *thin-ply composites, foldable structures, biomedical application, hybrid composites*

ABSTRACT

Thin-ply composite materials have demonstrated potential for use in high-performance applications requiring superior stiffness and specific strength. Self-expandable carbon fiber composite structures have been proposed for use in cardiovascular implants as transcatheter heart valve stents, which can be packaged to less than half their original diameter. However, the demands of such devices require increased foldability, which may be achieved by leveraging the elasticity of glass fibers. In this study, thin-ply glass fiber/epoxy composites under bending loads, are shown to achieve nominal maximum strains of 4.3%, which approaches the theoretical limit of glass fibers. As the demands of flexibility and stiffness may vary per direction, hybrid glass and carbon fiber layups are also investigated. Results show that glass fiber composite materials have considerable promise for use in not only transcatheter heart valve stents, but also other high-performance applications that require a balance between not only high flexibility and strains, stiffness, but also specific strength.

1 Introduction

Recent advances in prepreg production have allowed for the manufacturing of high quality, low areal weight (<20 g/m^2) thin-ply materials [1]. Despite requiring increased manufacturing effort due to higher complexity, thin-ply materials can be leveraged in high-performance applications for improved structure stiffness and strength [2]. Unidirectional (UD) carbon fiber (CF) thin-ply structures have been shown to accommodate very small bending radii of ~2 mm and elastic compressive strains of up to 3% without compressive micro-buckling [3]. At such low thicknesses, tensile fiber failure is expected to drive ultimate failure, rather than micro-buckling [4]. The fiber nanostructure of thin-ply structures can therefore accommodate much higher elastic strains compared to conventional materials such as metals, which can barely reach elastic strains of 1% [5]. Furthermore, the *in-situ* shear strength of laminates has been shown to increase greatly when ply thickness decreases [6].

However, by leveraging materials with more extended elastic regimes, even higher strains can be realized. This degree of resilience upon bending enables highly stowable and passively deployable space structures. For example, thin-ply composite materials have been proposed for common space structure components such as TRAC-booms [7]. Moreover, this function has been proposed in transcatheter heart valve stents, which utilize elastic packaging and expansion upon delivery. CF composite stents capable of expanding from diameters of 12 mm to 29 mm have been reported, which offer continuous interfaces in contrast to the metal mesh stents currently used in commercial devices [8]. This stent design eliminates the stress concentrations found in state-of-the-art devices, which has positive implications for the durability of composite-based transcatheter heart valve implants, such as those shown in Figure 1. However, the use of composites for such applications requires even smaller bending radii [9].

Figure 1: Top (left) and side (right) view of heart valve implants with carbon fiber composite stents

The scope of this work is to investigate the potential of highly elastic fibers, namely glass fiber (GF), to expand the design space for the aforementioned applications. Hybrid composite layups will be investigated to optimize the interplay between high bending strain (on a major direction) and transverse stiffness (on the secondary one). The bending radii achieved by layups of thickness < 130 µm will be experimentally determined. Furthermore, modeling based on composite laminate theory will be performed to assess the failure mechanism for each layup. From this study, we demonstrate the potential of GF and GF/CF hybrid composite thin-ply materials for transcathether heart valve stents as well as applications in aerospace and beyond.

2 Manufacturing of glass fiber/epoxy and carbon fiber/epoxy thin-ply materials

Large strain bending tests were performed on glass and carbon fiber epoxy thin-ply shells to characterize their bending behaviour. The specimens were manufactured using a 25 g/m^2 unidirectional e-glass/ThinPreg^{TM} 402 and a 20 g/m^2 unidirectional Toray T700S carbon fiber/ThinPreg^{TM} 513 prepreg. To improve transverse stiffness, GF and CF mid-layers were incorporated into the layups. In addition to unidirectional GF (GF_{UD}), layups containing GF angled-plies ($GF_{UD\text{-}AP}$), GF cross-plies ($GF_{UD\text{-}CP}$), CF angle-plies (GF_{UD}-CF_{AP}), and CF cross-plies (GF_{UD}-CF_{CP}) were investigated. A summary of the layups investigated is displayed in Table 1. The angled and cross-ply layups will be essential for the desired heart valve application given that the valve should have some acceptable stiffness in the flow direction in addition to the radial stiffness acting in the aortic tissue.

Flat composite layups were consolidated in an autoclave on an aluminum plate covered with polyimide release foil at a temperature of 135°C and pressure of 3 bar for 2 hours. Coupons of size 100×40mm were cut from the manufactured thin plates. On average, the specimens had nominal thicknesses between 111-127 µm. The somewhat decreased thickness for GF_{UD} compared to $GF_{UD\text{-}AP}$ and $GF_{UD\text{-}CP}$ can be attributed to more efficient fiber packing due to lack of fiber crossing. Figure 2 shows micrographs for each sample.

Sample	Layup	Thickness, t_{shell}
GF_{UD}	$[0]_{6,GF}$	111 µm
$GF_{UD\text{-}AP}$	$[0_{2,GF}/\text{-}45_{GF}/+45_{GF}/0_{2,GF}]$	115 µm
$GF_{UD\text{-}CP}$	$[0_{2,GF}/90_{2,GF}/0_{2,GF}]$	119 µm
GF_{UD}-CF_{AP}	$[0_{2,GF}/\text{-}45_{CF}/+45_{CF}/0_{2,GF}]$	127 µm
GF_{UD}-CF_{CP}	$[0_{2,GF}/90_{2,CF}/0_{2,GF}]$	126 µm

Table 1: Summary of manufactured layups

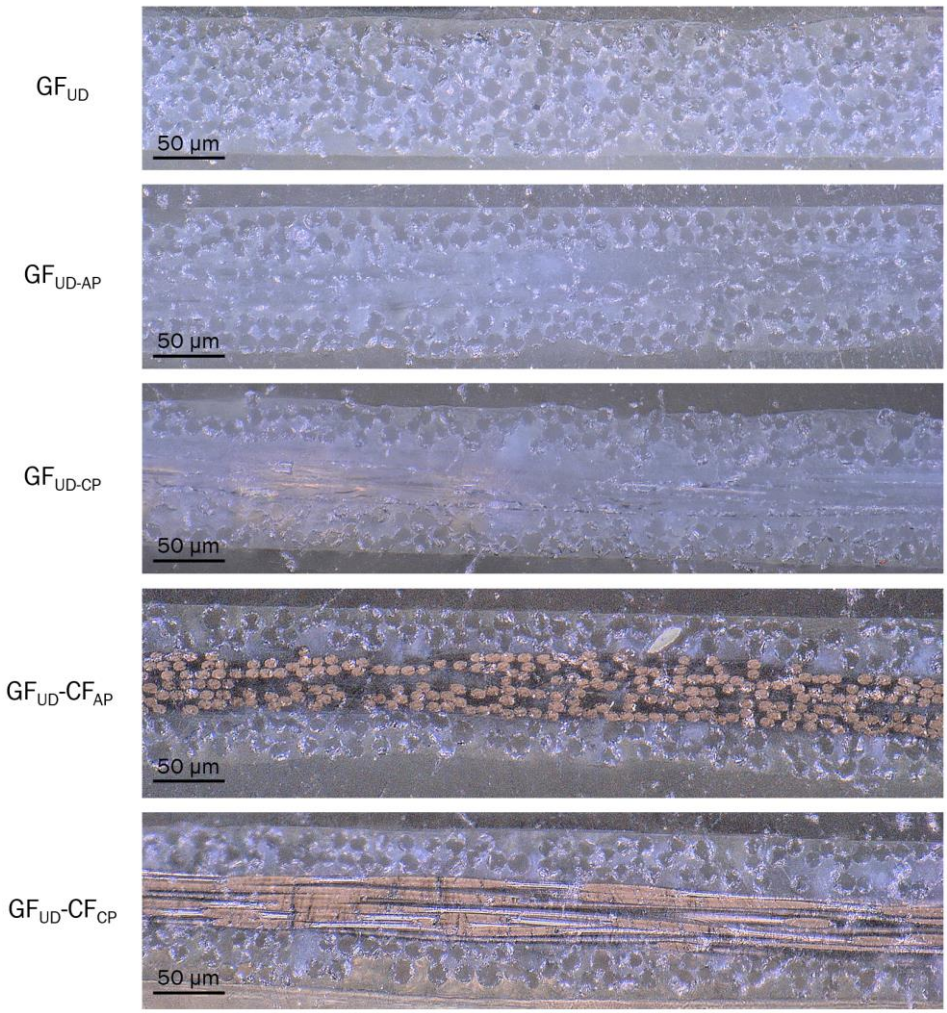

Figure 2: Cross-section micrographs of manufactured layups. Note the transparency of GF compared to the high reflection of CF.

3 Mechanical testing of thin-ply glass fiber materials

To measure bending failure strains, flat composite samples were folded into a U-shape following a shell buckling configuration being compressed between parallel platens until failure (Fig. 3a) [10]. The testing was performed with a Zwick Roell 1474 RetroLine testing machine and a 5 kN load cell at a displacement rate of 10 mm min^{-1}. Plates were slightly pre-buckled in the desired direction prior to testing. The displacement was used to determine the achieved bending radii (Fig. 3b), assuming cylindrical bending conditions and uniform curvature given the results of previous studies [3]. To calculate nominal strain values, we used the Bernoulli bending equation with a linear strain distribution through thickness (Eq. 1):

$$\epsilon = \frac{\kappa t_{shell}}{2} \tag{1}$$

Where ϵ is the strain, κ is the curvature, and t_{shell} is the plate thickness [4]. By combining large deformation mechanical testing and microscopic structural analysis, we can investigate the elastic limits of glass fiber-reinforced thin-ply composites. Generally, the GF$_{UD}$ specimens can reach higher deformations prior to break compared to the other samples, followed by GF$_{UD}$-CF$_{CP}$ specimens. Kinks in the load-deformation curves indicate failure of the first lamina, also known as first-ply failure (FPF), which have been labelled in Figure 3b.

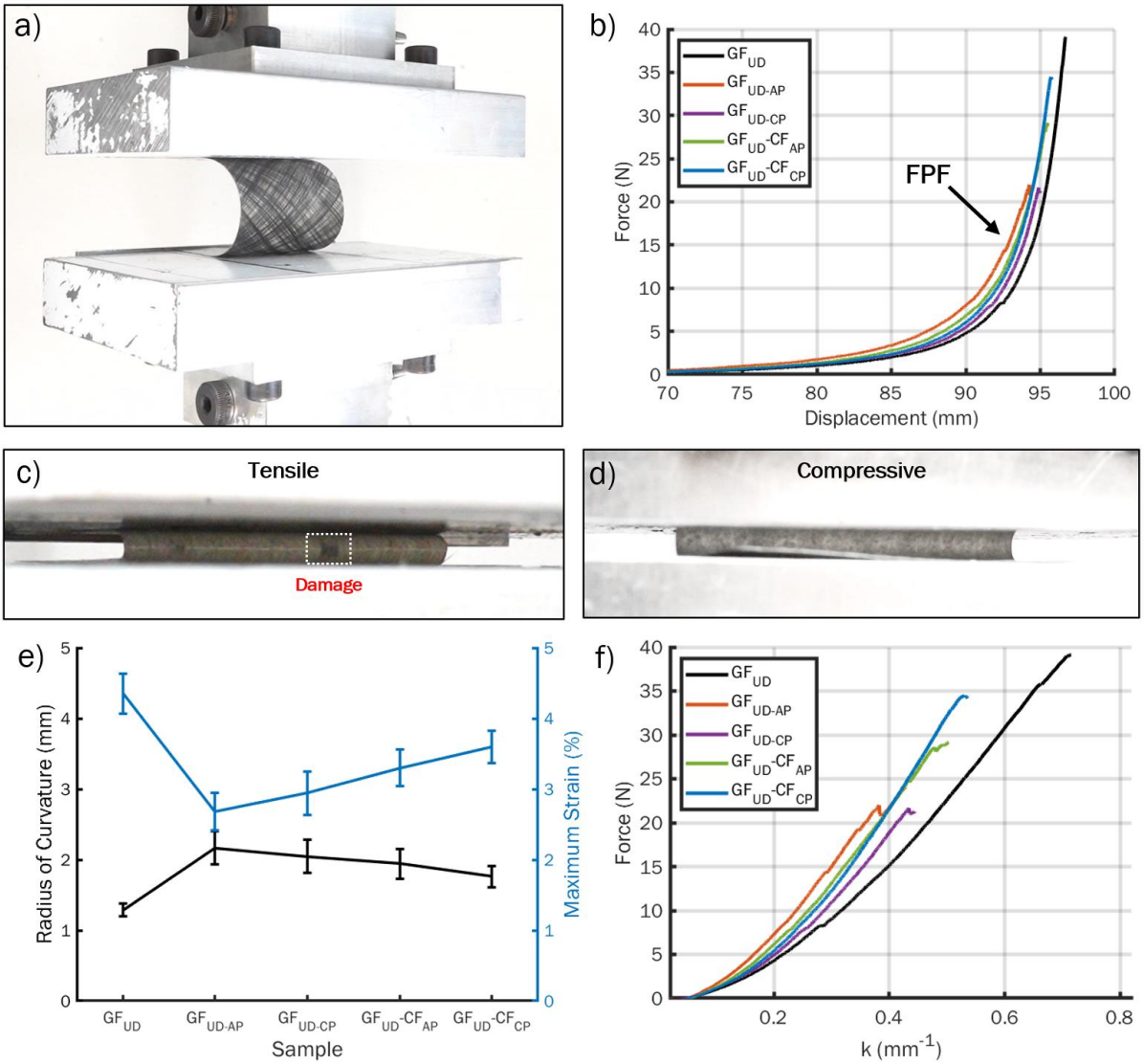

Figure 3: a) Image demonstrating platen test in progress and b) representative force-displacement curves obtained for all samples, where 100 mm of displacement corresponds to zero radius of curvature. An arrow notes first ply failure observed for $GF_{UD\text{-}AP}$. Images of visible failure in GF_{UD} taken at a curvature of 0.7 mm^{-1} on the c) tensile and d) compressive side. e) Radius of curvature (mm) and nominal maximum strain (%) values obtained for all samples. f) Nominal curvature κ (mm^{-1}) plotted against force.

Figure 3b shows that bending radii of 1.29 mm can be achieved for the 0.11 m thick UD GF-reinforced composites when taking advantage of glass fiber linear elasticity. Comparable 0.13 mm thick UD CF specimens were reported to have bending radii of 2.3 mm, nearly twice that of the GF_{UD} specimens [4]. The difference in performance can be attributed to the extended linear regime of glass fibers. Furthermore, Fig. 3c-d show that while damage on the tensile side can be observed in GF_{UD} at a curvature of 0.7 mm^{-1}, there is no visible damage on the compressive side, confirming the absence of previously described compressive micro-buckling [3], [4]. The GF_{UD} structures demonstrated nominal maximum strain of 4.3% (Fig. 3e) based on the evaluated curvature, which approaches the theoretical strain limits of e-glass [5].

Table 2 displays a summary of the performance for each investigated layup. From the force-displacement curves, we can observe that the addition of angled- and cross-plies leads to first-ply failure in the central plies, as well as nominal maximum bending strains at break between 2.7 and 3.6%. These

materials already show higher flexibility than the previously reported CF-based thin-ply composites [9]. Part of this high performance is attributed this to the *in-situ* strength effect observed with decreasing ply thickness [6]. The angled-ply stacking typically showed some slight yielding before ultimate failure, while the failure is more abrupt on the GF_{UD} and cross-ply samples attributed to the effect of shear. Note that for GF_{UD}, ultimate failure is often preceded by some minor damage in the range of 4.1%, identified by a kink in the force-displacement curve.

Generally, samples with cross-ply mid-layers could reach higher curvatures compared to samples with angled-ply mid-layers. This is likely due to the combination of shear and transverse stresses due to the stacking sequence.

Sample	Stain at break, ε_{break}	Bending Radii at break, r_{break}	Curvature at break, κ_{break}	Strain at FPF, ε_{FPF}	Bending Radii at FPF, r_{FPF}	Curvature at FPF, κ_{FPF}
GF_{UD}	4.3%	1.29 mm	0.78 mm^{-1}	4.1%	1.41 mm	0.71 mm^{-1}
$GF_{UD\text{-}AP}$	2.7%	2.17 mm	0.46 mm^{-1}	2.2%	2.59 mm	0.43 mm^{-1}
$GF_{UD\text{-}CP}$	2.9%	2.05 mm	0.49 mm^{-1}	2.8%	2.17 mm	0.46 mm^{-1}
GF_{UD}-CF_{AP}	3.3%	1.94 mm	0.52 mm^{-1}	3.0%	2.09 mm	0.48 mm^{-1}
GF_{UD}-CF_{CP}	3.6%	1.76 mm	0.57 mm^{-1}	3.3%	1.93 mm	0.52 mm^{-1}

Table 2: Summary of layup performance with mean values from 4 samples per family

On average, layups incorporating carbon fiber mid-layers showed significantly higher strain at break and at first ply failure compared with their glass fiber equivalents. The GF_{UD}-CF_{AP} and GF_{UD}-CF_{CP} samples could reach bending radii less than 2 mm while the $GF_{UD\text{-}AP}$ and $GF_{UD\text{-}CP}$ samples failed beforehand. Recent studies in hybrid glass/carbon/epoxy composites have shown a synergistic relationship when combining glass fiber/epoxy and carbon fiber/epoxy interfaces [11]. Strong Lewis acid-base interactions between carbon fiber and the epoxy matrix result in high interfacial energy, indicating high energies required for delamination [11]. Conversely, for glass fiber/epoxy composites, organosilane binding agents are required to promote bonding between the glass fiber and epoxy matrix. These silane binders are largely responsible for interfacial interactions and silane bonds confer high toughness to laminates, improving fracture toughness [11]–[13].

4 Large strain bending stress modeling

The local stress distributions in fiber (-11-) and transverse to the fiber direction (-22-) of each layup were simulated using the eLamX open-source software developed at Technische Universität Dresden, Institute of Aerospace Engineering, Chair of Aircraft Engineering. Curvatures of $\kappa = 0.33$ and 0.5 mm^{-1} were applied, corresponding to bending radii of 3 and 2 mm, respectively, in addition to curvatures at break and first ply failure. As shown in Figure 4, a continuous stress distribution was predicted for the GF_{UD}. Failure would ordinarily be expected for ply 6 *via* compressive fiber failure, yet the absence of compressive micro-buckling in thin ply composites allows for even higher strains before break.

For $GF_{UD\text{-}AP}$, significant transverse (max. 56.1 MPa) and shear stresses (max. 38.0 MPa) in ply 3 were introduced. These transverse stresses can cause transverse cracking related to fiber-matrix interface failure, but also shear matrix yielding [14], [15]. This is demonstrated by the experimental results, which show reduced strain at break compared to the GF_{UD}. With the addition of cross-ply layers, even higher transverse stresses (max. 85.7 MPa) are predicted in plies 3 and 4. For $GF_{UD\text{-}CP}$, high transverse stresses in ply 3 are expected to contribute to failure.

When compared with $GF_{UD\text{-}AP}$, comparable transverse (max. 54.3 MPa) and increased shear stresses (max. 48.0 MPa) are expected in plies 3 and 4 in GF_{UD}-CF_{AP}. Ultimately, the combined shear and transverse strains likely also cause failure in GF_{UD}-CF_{AP} specimens. Generally, the carbon fiber-epoxy interface bears the load more successfully than the glass fiber counterpart, which is reflected in the higher curvatures experimentally determined for GF_{UD}-CF_{AP}.

Figure 4: Local stress distributions and layup diagrams for the a) GF_{UD}, b) $GF_{UD\text{-}AP}$, c) $GF_{UD\text{-}CP}$, d) GF_{UD}-CF_{AP}, and e) GF_{UD}-CF_{CP} specimens

Slightly higher normal transverse stresses (95.2 MPa) are also present in the cross-ply layers for GF_{UD}-CF_{CP} compared to $GF_{UD\text{-}CP}$. However, the superior carbon fiber-epoxy interface results in superior performance for GF_{UD}-CF_{CP} which is shown in the higher strain at first ply failure and break. Furthermore, the layup is predicted to have by far the highest transverse flexural modulus amongst all layups. In general, cross-ply layups appear to withstand higher curvatures than angled-ply layups, and layups with carbon fiber mid-layers fare better than those with glass-fiber mid-layers. In all cases, the in-situ strength effect [6] has a significant influence as the expected transverse tensile inter-fiber stresses at break are much higher than the literature value (23 MPa) for that of pure UD [2].

To compare the performance between angled and cross-ply samples, the tensile inter-fiber Hashin criteria were also calculated to evaluate the likelihood of failure (Eq. 2):

$$\left(\frac{\sigma_{22}+\sigma_{33}}{Y_T}\right)^2+\frac{\tau_{23}^2-\sigma_{22}\sigma_{33}}{S_Q^2}+\frac{\tau_{12}^2+\tau_{13}^2}{S_L^2}=1 \quad (2)$$

Where Y_T, S_L, and S_Q are the strength limits for stresses $\sigma_{22,33}$, $\tau_{12,13}$, and τ_{23}, respectively [17]. Since samples were approximated with Classical Laminate Theory (CLT), all through-thickness values were neglected, resulting in Eq. 3:

$$\left(\frac{\sigma_{22}}{Y_T}\right)^2+\frac{\tau_{12}^2}{S_L^2}=1 \quad (3)$$

Due to the absence of compressive micro-buckling at such low thicknesses the only failure expected in fiber direction is tensile. Regarding the transverse tensile case, Y_T was calculated from the σ_{22} at break simulated for cross-ply samples (i.e., 95.2 MPa for CF and 85.7 for GF), and S_L was calculated from Y_T values and the τ_{12} at break simulated for angled-ply samples. Table 3 summarizes the analysis, as well as effective laminate in plane and flexural moduli that were also calculated. By calculating the Hashin criteria at curvatures of 0.33 mm^{-1} and 0.5 mm^{-1}, we see that the likelihood of failure is generally much higher with the angled-plies, due to the combination of shear and transverse stresses. The experimental results are in good agreement with the calculated Hashin criteria, predicting no failure at a curvature of 0.33 mm^{-1}. In agreement with experimental results, failure was also predicted at a curvature of 0.5 mm^{-1} for samples $GF_{UD\text{-}AP}$ and $GF_{UD\text{-}CP}$.

Sample	Hashin Criteria at $\kappa = 0.33\ mm^{-1}$	Hashin Criteria at $\kappa = 0.5\ mm^{-1}$	$\bar{E}_x$ (GPa)	$\bar{E}_y$ (GPa)	$\bar{G}_{xy}$ (GPa)	$\bar{E}_x^f$ (GPa)	$\bar{E}_y^f$ (GPa)	$\bar{G}_{xy}^f$ (GPa)
GF_{UD}	0.158	0.363	39.0	8.6	3.8	39.0	8.6	3.8
$GF_{UD\text{-}AP}$	0.538	1.235	30.1	10.7	6.1	38.0	8.8	4.0
$GF_{UD\text{-}CP}$	0.454	1.041	29.1	18.9	4.1	37.9	9.7	3.8
GF_{UD}-CF_{AP}	0.388	0.890	32.2	14.7	12.2	38.2	9.1	4.4
GF_{UD}-CF_{CP}	0.335	0.845	29.1	46.9	4.1	38.1	12.9	3.8

Table 3: Calculated Hashin criteria (only including the transverse tensile case) as well as homogenized in-plane and flexural moduli for manufactured layups, where orange and green are used to indicate where failure is predicted and not predicted, respectively.

5 Conclusions

As previously mentioned, highly foldable and stiff thin-ply composite structures have many potential applications including cardiovascular implants, namely transcatheter heart valve stents. Self-deployable CF-reinforced composite cylinders that can be compressed from a diameter of 29 mm to 12 mm were previously reported, however a further decrease in the radii is required for catheter delivery [9]. Our work highlights the potential for glass fiber-reinforced thin-ply materials in such an application. We experimentally demonstrate bending radii as small as 1.29 mm for such glass fiber-based materials and show that it is possible to balance high strain with stiffness by using hybrid glass and carbon fiber composites, which is essential for transcatheter heart valve stents. The combination of experimental work with modeling further reveals the advantages of hybrid composite materials and guides the design of such materials. Future work would include replacing the epoxy-based matrix of these structures with a PEEK matrix to further enhance the material ductility and stiffness.

Acknowledgements

This work was partially funded by the ETHeart initiative from the Open ETH program by the Executive Board of ETH Zurich and the Zurich Heart project of Hochschulmedizin Zürich.

References

[1] S. Sihn, R. Y. Kim, K. Kawabe, and S. W. Tsai, "Experimental studies of thin-ply laminated composites," *Compos. Sci. Technol.*, vol. 67, no. 6, pp. 996–1008, 2007, doi: 10.1016/j.compscitech.2006.06.008.

[2] R. Amacher, J. Cugnoni, J. Botsis, L. Sorensen, W. Smith, and C. Dransfeld, "Thin ply composites: Experimental characterization and modeling of size-effects," *Compos. Sci. Technol.*, vol. 101, pp. 121–132, 2014, doi: 10.1016/j.compscitech.2014.06.027.

[3] A. Schlothauer, G. A. Pappas, and P. Ermanni, "Material response and failure of highly deformable carbon fiber composite shells," *Compos. Sci. Technol.*, vol. 199, no. July, p. 108378, 2020, doi: 10.1016/j.compscitech.2020.108378.

[4] G. A. Pappas, A. Schlothauer, and P. Ermanni, "Bending failure analysis and modeling of thin fiber reinforced shells," *Compos. Sci. Technol.*, vol. 216, p. 108979Pelzmühletal, 2021, doi: 10.1016/j.compscitech.2021.108979.

[5] I. M. Daniel and O. Ishai, *Engineering Mechanics of Composite Materials*, vol. 219. 2006.

[6] P. P. Camanho, C. G. Dávila, S. T. Pinho, L. Iannucci, and P. Robinson, "Prediction of in situ strengths and matrix cracking in composites under transverse tension and in-plane shear," *Compos. Part A Appl. Sci. Manuf.*, vol. 37, no. 2, pp. 165–176, 2006, doi: 10.1016/j.compositesa.2005.04.023.

[7] A. Schlothauer, N. Schwob, G. A. Pappas, and P. Ermanni, "Ultra-thin thermoplastic composites for foldable structures," *AIAA Scitech 2020 Forum*, vol. 1 PartF, no. January, pp. 1–12, 2020, doi: 10.2514/6.2020-0206.

[8] A. Schlothauer and P. Ermanni, "Stiff Composite Cylinders for Extremely Expandable Structures," *Sci. Rep.*, vol. 9, no. 1, pp. 1–6, 2019, doi: 10.1038/s41598-019-51529-7.

[9] A. Schlothauer and P. Ermanni, "Designing foldable composite structures on the micrometre scale," *ICCM Int. Conf. Compos. Mater.*, vol. 2019-Augus, 2019.

[10] G. Sanford, A. Biskner, T. Murphey, P. Engineer, P. Engineer, and S. V. Directorate, "Large strain behavior of thin unidirectional composite flexures," *Collect. Tech. Pap. - AIAA/ASME/ASCE/AHS/ASC Struct. Struct. Dyn. Mater. Conf.*, no. April, pp. 1–15, 2010, doi: 10.2514/6.2010-2698.

[11] F. Maciel, D. Daou, O. Pekovi, A. Simonovi, J. C. Voorwald, and M. Odila, "FEA simulation and experimental validation of mode I and II delamination at the carbon/glass/epoxy hybrid interface : Physical-based interpretation," *Compos. Commun.*, vol. 22, no. October, pp. 1–7, 2020, doi: 10.1016/j.coco.2020.100532.

[12] Y. Wan, L. Gong, L. Tang, L. Wu, and J. Jiang, "Mechanical properties of epoxy composites filled with silane-functionalized graphene oxide," *Compos. - Part A Appl. Sci. Manuf.*, vol. 64, pp. 79–89, 2014, doi: 10.1016/j.compositesa.2014.04.023.

[13] E. Feresenbet, D. Raghavan, and G. A. Holmes, "The influence of silane coupling agent composition on the surface characterization of fiber and on fiber-matrix interfacial shear strength," *J. Adhes.*, vol. 8464, 2010, doi: 10.1080/00218460309580.

[14] T. Rev, M. R. Wisnom, X. Xu, and G. Czél, "The effect of transverse compressive stresses on tensile failure of carbon fibre/epoxy composites," *Compos. Part A Appl. Sci. Manuf.*, vol. 156, no. November 2021, 2022, doi: 10.1016/j.compositesa.2022.106894.

[15] A. Schlothauer, "Resilient Thin Shell Composites for Extremely Deformable Structures," 2021.

[16] North Thin Ply Technology, "Data Sheet: NTPT Thinpreg 513." pp. 1–4, 2017.

[17] Z. Hashin, "Fatigue Failure Criteria for Unidirectional Fiber Composites," *Trans. ASME*, vol. 48, pp. 846–852, 1981.